

Instrument Concepts and Technologies for Future Spaceborne Atmospheric Radars

Eastwood Im* and Stephen L. Durden

Jet Propulsion Laboratory, California Institute of Technology, Pasadena, CA 91109, USA

ABSTRACT

In conjunction with the implementation of spaceborne atmospheric radar flight missions, NASA is developing advanced instrument concepts and technologies for future spaceborne atmosphere radars, with the over-arching objectives of making such instruments more capable in supporting future science needs, and more cost effective. Two such examples are the Second-Generation Precipitation Radar (PR-2) and the Nexrad-In-Space (NIS). PR-2 is a 14/35-GHz dual-frequency rain radar with a deployable 5-meter, wide-swath scanned membrane antenna, a dual-polarized/dual-frequency receiver, and a real-time digital signal processor. It is intended for Low Earth Orbit (LEO) operations to provide greatly enhanced rainfall profile retrieval accuracy while using only a fraction of the mass of the current TRMM PR. NIS is designed to be a 35-GHz Geostationary Earth Orbiting (GEO) radar with the intent of providing hourly monitoring of the life cycle of hurricanes and tropical storms. It uses a 35-m, spherical, lightweight membrane antenna and Doppler processing to acquire 3-dimensional information on the intensity and vertical motion of hurricane rainfall. Technologies for NIS are synergistic with those for PR-2. During the last two years, several of the technology items associated with these notional instruments have also been prototyped. This paper will give an overview of these instrument design concepts and their associated technologies.

Keywords: TRMM, GPM, PR-2, NIS, GEO, LEO, precipitation, rainfall, radar

1. INTRODUCTION

Atmospheric latent heating field is fundamental to all modes of atmospheric circulation and upper mixed layer ocean circulations. The key to understanding the atmospheric heating process is understanding where precipitation occurs. The atmospheric processes which link precipitation to atmospheric circulation include: (1) convective mass fluxes in the form of updrafts and downdrafts; (2) microphysical nucleation and growth of hydrometeors; and (3) latent heating through dynamical controls on the mass flux of precipitation. It is well-known that surface and rainfall are two of the key forcing functions on a number of geophysical parameters at the surface-air interface. Over ocean, rainfall variation contributes to the redistribution of water salinity, sea surface temperature, fresh water supply, and marine biology and eco-system. Over land, rainfall plays a significant role in rainforest ecology and chemistry, land hydrology and surface runoff. Precipitation has also been closely linked to a number of atmospheric anomalies and natural hazards that occur at various time scales, including hurricanes, cyclones, tropical depressions, flash floods, droughts, and most noticeable of all, the El Ninos. From this point of view, the significance of global atmospheric precipitation has gone far beyond the science arena - it has a far-reaching impact on human's socio-economic well-being and sustenance.

These and many other science applications require the knowledge of, on a global basis, the vertical rain structures, including vertical motion, rain intensity, differentiation of the precipitating hydrometeors' phase state, and the classification of mesoscale physical structure of the rain systems. The only direct means to obtain such information is the use of spaceborne profiling radars. It is important to mention that the Tropical Rainfall Measuring Mission¹ (TRMM) in the LEO has made a great stride forward towards this ultimate goal. The Precipitation Radar² (PR) aboard the TRMM satellite is the first-ever spaceborne radar dedicated to three-dimensional, global precipitation measurements over the tropics and the subtropics, as well as the detailed synopsis of a wide range of tropical rainstorm systems. The measurements collected by the PR, together with those collected by other science instruments aboard the TRMM satellite have provided unprecedented insights into the rainfall systems. It is anticipated that a lot more exciting and

* E-mail: eastwood.im@jpl.nasa.gov; Phone: 1-818-354-0492

important rain observations would be made by TRMM for the remaining of its mission duration.

While TRMM has provided invaluable data to the user community, it is only the first step towards advancing our knowledge on rain processes and its contributions to climate variability. A follow-on LEO mission, called the Global Precipitation Mission³ (GPM), is currently being developed to capitalize on the pioneering information provided by TRMM, and to extend the TRMM's instrument capability in such a way to fully address the key science questions from microphysical to climatic time scale. Another key science component of GPM is the study the global hydrological cycle. The baseline GPM instrument configuration consists of a constellation of several micro-satellites each carries a 3-frequency scanning radiometer, and a core satellite which carries a 5-frequency scanning radiometer, and a 14-GHz scanning radar and a 35-GHz scanning radar working in a synchronized and matched-beam fashion. The suite of radiometers is intended to provide a global, 3-hourly data set for hydrological applications and numerical weather prediction, and the two radars are intended to provide detailed observations of rainfall processes and microphysics. To support the instrument technology development and fusion to future NASA science missions such as GPM, a notional instrument concept, using a dual-frequency rain radar with a deployable 5-meter electronically-scanned membrane antenna and real-time digital signal processing, is developed. This new system, the Second Generation Precipitation Radar (PR-2), has the potential of offering greatly enhanced performance accuracy while using only a fraction of the mass of the current TRMM PR.

In parallel with the LEO PR-2 technology development, NASA has initiated an instrument definition study and some advanced technology development for a notional geostationary orbiting atmospheric radar, the Nexrad-In-Space (NIS), for detailed monitoring of hurricanes. Radar remote sensing of the atmosphere and severe storms from geostationary orbit is highly desirable owing to the radar's unique ability to penetrate precipitating clouds and to simultaneously provide vertical rainfall profiles, large spatial coverage, and frequent observations. The observations made with such instrument will enable hurricane rain and cloud processes to be monitored over much of their life cycle, thus providing the temporal information needed for creating advanced flood and hazard warning systems, improving numerical model prediction of hurricane tracks and landfalls, and understanding more about the hurricane diurnal cycle.

During the last several years, several of the technology items associated with these two notional instruments have been prototyped. In this paper, the science rationales, the instrument design concept, and the technology status for these notional systems will be presented.

2. LEO ATMOSPHERIC RADAR INSTRUMENT CONCEPT AND TECHNOLOGY

The key PR-2 radar system design concept includes the following capabilities:

- a 14/35 GHz dual frequency radar electronics with Doppler and dual-polarization capabilities which allow more accurate rainfall rate retrievals and enable new ability to study the rainfall dynamics and microphysics;
- a large but light weight, dual-frequency, wide-swath scanning, deployable antenna which enables measurements at higher spatial resolution and reduces contamination from surface clutters;
- digital chirp generation and the corresponding on-board pulse compression scheme to allow a significant improvement on rain signal detection without using the traditional, high-peak-power transmitters and without sacrificing the range resolution;
- radar electronics and algorithm to adaptively scan the antenna so that more time can be spent observing rain rather than clear air; and
- built-in flexibility on the radar parameters and timing control such that the same radar can be used by different future rain missions.

2.1 PR-2 Instrument Design Approach

The PR-2 is designed to operate at orbital altitudes (h) ranging between 400 and 750 km. It will have two nominal operational modes: the Wide-Swath Mode and the Nadir Doppler Mode. During Wide-Swath mode operations, the antenna will scan $\pm 37^\circ$ across-track at $h=400$ km, or $\pm 28^\circ$ at $h=750$ km. The corresponding ground swaths are 600 and 800 km, respectively. Both the HH-polarized and HV-polarized rain reflectivity profiles at 14 and 35 GHz will be measured simultaneously in this mode. The Nadir Doppler mode will acquire the vertical Doppler profiles of

precipitation at nadir if precipitation is detected in such regions. At 400-km altitude, the required radar antenna aperture will be 5.3 m in order to achieve a 2-km horizontal resolution at 14 GHz – the resolution comparable to typical scale size of convective storm cells. The antenna will be under-illuminated at 35 GHz in order to obtain the matched, 2-km horizontal resolution. In order to obtain sufficient number of independent samples per resolution cell (TRMM PR obtains 64 samples), the antenna size will be increased only to 7.3 m at 750 km altitude. The corresponding horizontal resolution in this case will be 2.7 km. The horizontal resolution at 35 GHz will be about a factor 3 better. The vertical resolution will be set at 250 m at all altitudes of operation, but the chirp bandwidth will be 5.3 MHz to allow an 8-fold increase in the number of independent samples. The chirp pulse duration will vary in order to secure sufficient signal-to-noise ratios at all altitudes. The set of PR-2 system parameters are summarized in Table 1.

Parameter	h = 400 km		h = 750 km	
	14 GHz	35 GHz	14 GHz	35 GHz
Polarization	HH, HV	HH, HV	HH, HV	HH, HV
Antenna effective diameter	5.3 m	2.1 m	7.4 m	2.9 m
Antenna gain	55 dBi	55 dBi	58 dBi	57 dBi
Antenna sidelobe	-30 dB	-30 dB	-30 dB	-30 dB
Polarization isolation	-25 dB	-25 dB	-25 dB	-25 dB
Peak power	200 W	50 W	200 W	50 W
Bandwidth	5.3 MHz	5.3 MHz	5.3 MHz	5.3 MHz
Pulsewidth	40 μ sec	40 μ sec	40 μ sec	40 μ sec
PRF at Wide-swath mode	2.73 KHz	2.73 KHz	2.01 KHz	2.01 KHz
PRF at Doppler mode	5 KHz	5 KHz	5 KHz	5 KHz
Wide-swath dwell time	0.29 sec	0.29 sec	0.39 sec	0.39 sec
Doppler integration time	0.05 sec	0.05 sec	0.05 sec	0.05 sec
Vertical resolution	250 m	250 m	250 m	250 m
Horizontal resolution (nadir)	2 km	2 km	2.7 km	2.7 km
Ground swath	600 km	600 km	800 km	800 km
Independent samples	64	64	64	64
Min. detectable Zeq (after averaging)	5.0 dBZ	4.8 dBZ	6.7 dBZ	5.6 dBZ
Vertical Doppler accuracy	1 m/s	0.9 m/s	1 m/s	0.9 m/s

Table 1: PR-2 radar systems and performance parameters.

Wide Swath Mode: In this mode, rain reflectivity profiles will be measured over a large cross-track swath using the so-called ‘adaptive scan’ scheme. The designed antenna scan angle range would cover ground swaths ranging between 600 km at 400 km altitude and 800 km at 750 km altitude. As shown by the GATE results, the probability of rain occurrence over a specific location is < 20%. For this reason, and to effectively utilize the limited observation time, each PR-2 observation sequence will be divided into two periods: a Quick-Scan Period to determine the location and vertical extent of the rain cells within the entire swath, and a Dwell Period at which detailed precipitation measurements of the identified rain cells will be made. For example, at h = 400 km, a nominal observation sequence will last ~0.29 sec, the Quick-Scan Period will occupy the first 0.09 sec and the Dwell Period will use the remaining available time (0.2 sec). During the Quick-Scan Period the radar system will make a complete cross-track scan through the 600-km swath, transmit and receive only 1 pulse at each 2-km ground resolution cell at a nominal pulse repetition frequency (PRF) of 2730. The radar backscatter measurements at each resolution cell will be averaged on-board over a vertical column of 2 km (~64 samples) and will be compared with a set of thresholds and ranked according to their respective backscatter strength. The ranked results will then be used to develop the subsequent antenna scan pattern for the Dwell Period. In the Dwell Period, the radar will measure the detailed rain backscatter profile over areas with significant rainfall. The nominal swath covered in the Dwell Period is ~200 km, which should be sufficient to cover most of the rain areas within the swath. In the event that there is pervasive rainfall covering areas >200 km cross-track, our proposed dwell pattern would allow observations over cells with the most intense rainfall, thus covering a significant portion of the total rainfall in those areas. On-board processing will include pulse compression and range bin averaging.

Nadir Doppler Mode: When the Quick-Scan results indicate rain occurrence at or near nadir, the Nadir Doppler Mode will be exercised. In this mode, the radar antenna will be pointed at this small region for a total time of ~ 0.05 sec. A higher pulse repetition frequency (~ 5000) will be used to accommodate the anticipated Doppler spread. Multiple rain echoes obtained in each resolution cell will be used to estimate the Doppler shift caused by the mean rainfall motion. The mean vertical rainfall motion can be measured to an accuracy of about 1 m/s.

Detection Sensitivity: Figure 1 shows the signal-to-noise ratios (SNRs) of the like-polarized rain echoes as a function of the rain rate for the PR-2 system. Notice the significant sensitivity improvement, as compared to the TRMM PR, in detecting both very light rain (< 0.1 mm/hr) and very intense rain (~ 90 mm/hr) systems. At rain rates below ~ 15 mm/hr, measurements from both frequencies can be combined to measure the entire rain rate profile. At rain rates between 15 and 35 mm/hr, the dual-frequency measurements can be used to retrieve at least the upper half of the rain clouds. Furthermore, this figure illustrates that there will be sufficient sensitivity for the PR-2 to measure cross-polarized returns at rain rates ≥ 0.2 mm/hr.

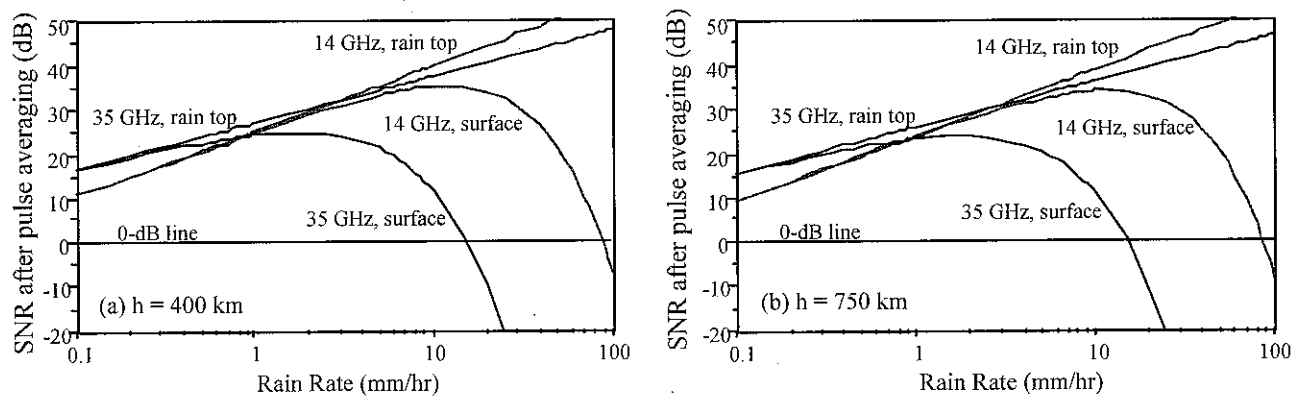


Fig. 1: Expected signal-to-noise ratios of the like-polarized rain returns for the PR-2 system and for radar altitudes of: (a) 400 km, and (b) 750 km. The rain top is assumed to be at an altitude of 5 km.

2.2 Radio-Frequency electronics subsystem

The PR-2 RF electronics subsystem consists of a NCO-based digital chirp generator (DCG) used to synthesize the chirp waveform, an upconverter and four receiver channels. The DCG approach, as demonstrated by ARMAR⁴ has the benefit of great flexibility in generating the shaped, linearly frequency-modulated pulses with sidelobe levels below -60 dB. The chirp waveform is generated at an IF frequency and upconverted to both Ku-band (14 GHz) and Ka-band (35 GHz) using a two-stage mixing process. The LO frequencies are provided by phase-locked oscillators and dielectric resonator oscillators, which are all locked to a reference oscillator for coherent up and downconversion, as is required for the Doppler mode. The signals are amplified to the desired radiated powers using the 14 and 35 GHz traveling wave tube amplifiers (TWTA) and transmitted through an ortho-mode transducer (OMT) and a circulator assembly to the dual-frequency antenna. The OMT and circulator are used to separate the horizontal and vertical polarization components at each frequency. A small amount of power in the transmit pulse is also directly coupled to the receiver channels to calibrate the sensitivity of the system and to accurately measure receiver gain and noise floor, which are essential to achieve the sensitivity and accuracy requirements of the system. There are four receiver channels, two required for 14 GHz (H- and V-pol) and two for 35 GHz (H- and V-pol). The receiver amplifies the returned echo using a low noise amplifier and coherently downconverts the signal to offset video.

The PR-2 LO/IF module is designed to be compact and flight qualifiable. The prototype model of this module, as shown in Figure 2, fits in 2 VME card slots and weighs 3.6 kg. Owing to its compact configuration, it is easily accessible for serviceability during testing, and is easy to be reconfigured for use by multiple missions. It has very good EMC characteristics with thorough sub-circuit shielding, and is conduction cooled.

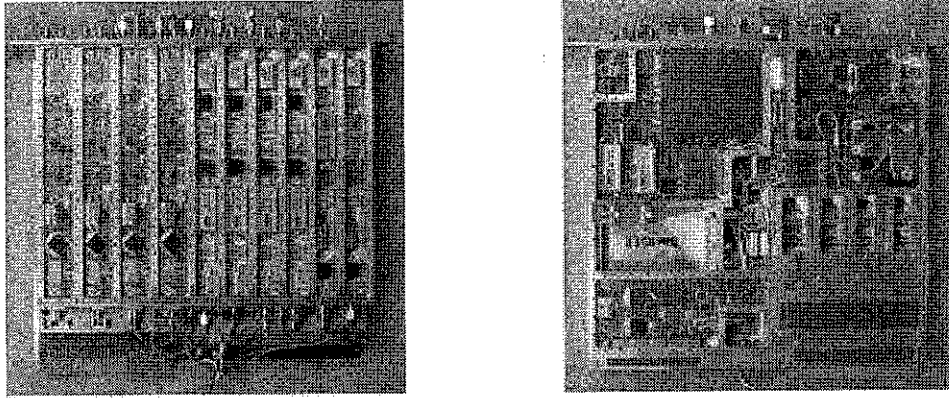


Fig. 2: Front- and back-side of the PR-2 LO/IF module prototype unit.

2.3 Digital electronics subsystem and real-time processor

The digital electronics subsystem consists of the control and timing unit (CTU), analog-to-digital converters (ADCs) for the four receiver channels, multiplexer, data processor, and data formatter. The control and timing unit decodes all radar mode commands, generates the required timing signals, and controls the timing of the antenna beam scan. The 12-bit ADCs, with dynamic range greater than 70 dB, digitize the linearly detected video signals. The digitized data is multiplexed and sent to the onboard data processor. The data processor performs digital pulse compression, range bin averaging, ranking of the data acquired in the Quick-Scan Period to determine rain locations, and Doppler processing. The processed data are formatted and sent to the tape recorder for storage.

Digital pulse compression techniques permit compensation for non-ideal characteristics of the system (provided that they are well characterized) and can provide substantially better sidelobe suppression than the analog pulse compression using dispersive filters such as surface acoustic wave devices (SAW). Experiments with ARMAR⁴ demonstrated sidelobe suppression of up to 60 dB. However, this was achieved by recording all radar echoes on a high-speed tape recorder and processing them later. For spaceborne operations, however, it is not practical to downlink large volumes of raw echo data, a real time processing solution is required.

The PR-2's real-time digital pulse compression technology has been demonstrated by the development of the airborne prototype model. This model uses a combination of custom and commercial-off-the-shelf (COTS) VME hardware. The system has two main components, a four-channel (two received polarizations by two frequencies) acquisition board and a programmable digital signal processor board which uses Xilinx field programmable gate arrays (FPGAs).

The PR-2 airborne prototype uses a custom 12 bit analog-to-digital converter (ADC) board based on an Analog Devices 14 bit converter, which provides four simultaneously sampled and processed channels (14- and 35-GHz, H and V receive channels). Data is oversampled a factor of 2 above Nyquist limit and then digitally low-pass filtered and decimated by a factor of two. Using a digital filter as the main video filter, allows more precise control of the filter characteristics and eases the requirements on the analog antialiasing filter.

The real-time signal processor card shown in Figure 3 is a COTS VME card made by Annapolis Microsystems. The board contains three large Xilinx Vertex FPGAs; reprogrammable parts which can be configured as almost any kind of digital logic. With four channels, the system performs 20 billion multiplications and 20 billion additions per second. This processing throughput would be difficult to achieve with microprocessors. FPGAs enable implementation of efficient and algorithm-specific circuitry without the nonrecurring costs and development time associated with application specific integrated circuits (ASICs). The highly parallel implementations possible with FPGAs allow realization of the entire real-time processor in only two chips.

The front-end of the processor is four 64-tap, 16-bit finite impulse response (FIR) filters implemented with bit serial multipliers clocking at 133 MHz. The filter receives 20 MHz offset video, and selects 4 MHz flat bandwidth centered around 5 MHz, with 70 dB suppression of the 4 MHz band centered around DC. Following the filter is a downsampling and digital IQ demodulation yielding in-phase and quadrature baseband signals. The output data is complex and clocked

at 5 MHz. Following the video filter is a matched filter stage. This is a 256 tap complex FIR filter (actually 4 real integer FIR filters) loaded with a 12 bit reference function clocking at 5 MHz. The reference function we use is a Kaiser window ($K=6$) squared envelope modulated on an ideal chirp which has been modified slightly to tune out system distortion.

For every range sample the co- and cross-polarized echo power is computed. The pulse pair technique is used to calculate the Doppler velocity and the Doppler spectral width. The power and pulse-pair estimates from 64 pulses are then averaged, yielding a 64-fold reduction the output data rate. Any echo containing a saturated ADC value is dropped from the averages because even a single clipped ADC sample creates large sidelobes which can obscure much of the useful data near the oceans surface. The averaging and resulting reduction in data rate is only possible only after pulse compression and calculation of power and pulse-pair estimates has been performed.

The PR-2 prototype's pulse compression performance was evaluated during an airborne engineering test flight in which the nadir returns from the clear ocean were captured and processed in real time. Figure 4 shows an example of the output signals of the processor. This waveform is an average of 64 individual pulses. This figure demonstrates that the technique can indeed achieve sidelobe suppression of 60 dB as designed.

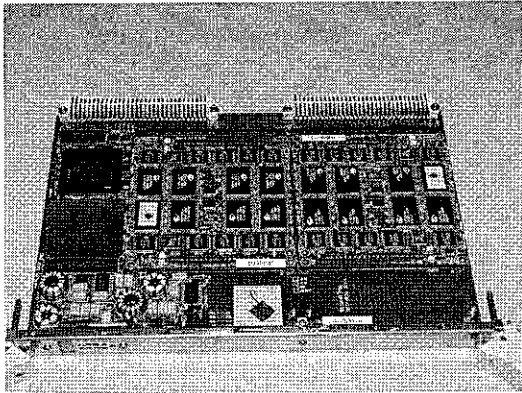


Fig. 3: FPGA-based PR-2 data processor.

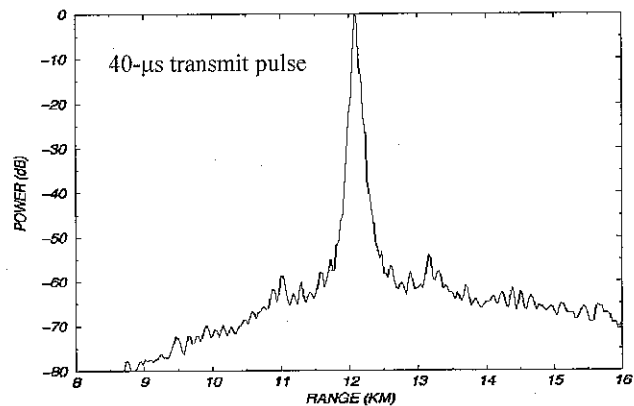


Fig. 4: Shape of a compressed signal from clear ocean. It consists of an average of 64 backscattered echoes.

2.4 Radar antenna

The large swath coverage and fine horizontal resolution desired for detailed rain profiling by radars lead to the use of a large (5 to 7 m diameter), dual-frequency, scanning antenna. while the TRMM PR type antenna design can be extended to a larger scan range and to two frequencies, its rigid structure would be too heavy and cannot be easily accommodated by typical, low-cost, satellite buses and launch vehicles. The PR-2 antenna, therefore, is designed to achieve the goals of low mass, small stowage volume, and low cost. We are currently studying a 5.3m x 5.3m cylindrical/parabolic inflatable antenna offset-fed by a linear array with T/R modules for spaceborne rain application at satellite altitude of 400 km. This antenna concept as graphically illustrated in Figure 5 is selected primarily because of its ability to achieve the wide-angle beam scanning in the required single plane. A conventional doubly curved parabolic reflector can only scan its main beam a few beamwidths away from its broadside direction. A linear array feed is used because it only requires N number of T/R modules instead of the required $N \times N$ number in the case of a planar array. Offset configuration is selected to avoid feed blockage and, thus, to achieve the required low sidelobe level (-30 dB). Figure 6 illustrates the under-illuminated reflector surface-current distribution due to the 35-GHz feed. In order to achieve the required matched

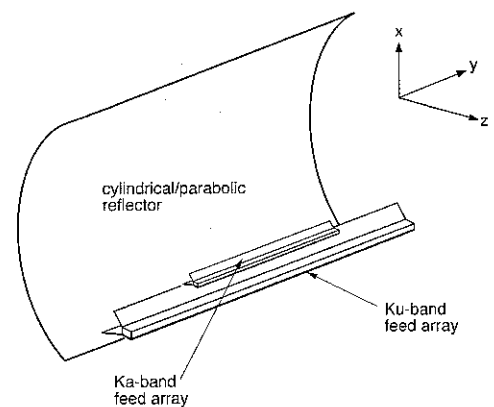


Fig. 5: Configuration of a cylindrical/ parabolic reflector illuminated by a linear array.

beams for the two frequencies, the 35-GHz feed needs to under-illuminate the reflector and be less than half the length of the 14-GHz feed.

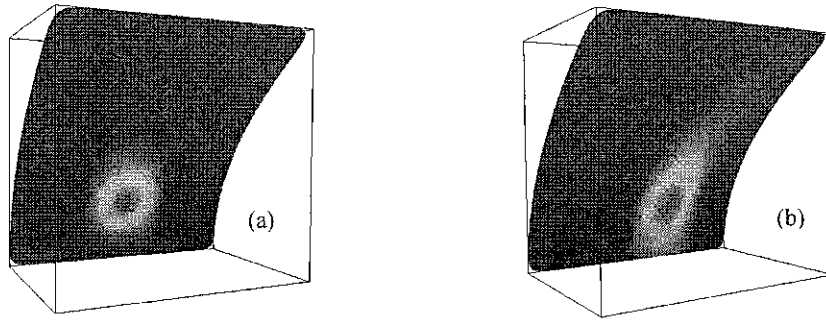


Fig. 6: Current distribution on reflector antenna surface for the 35-GHz case. (a) Beam at boresight. (b) Beam tilt to 20°.

Representative 14- and 35-GHz antenna directivity patterns, together with the required sidelobe level (green curves) are given in Figure 7. For the 37°-scanned beams, some beam widening can be observed, which may degrade the radar performance somewhat.

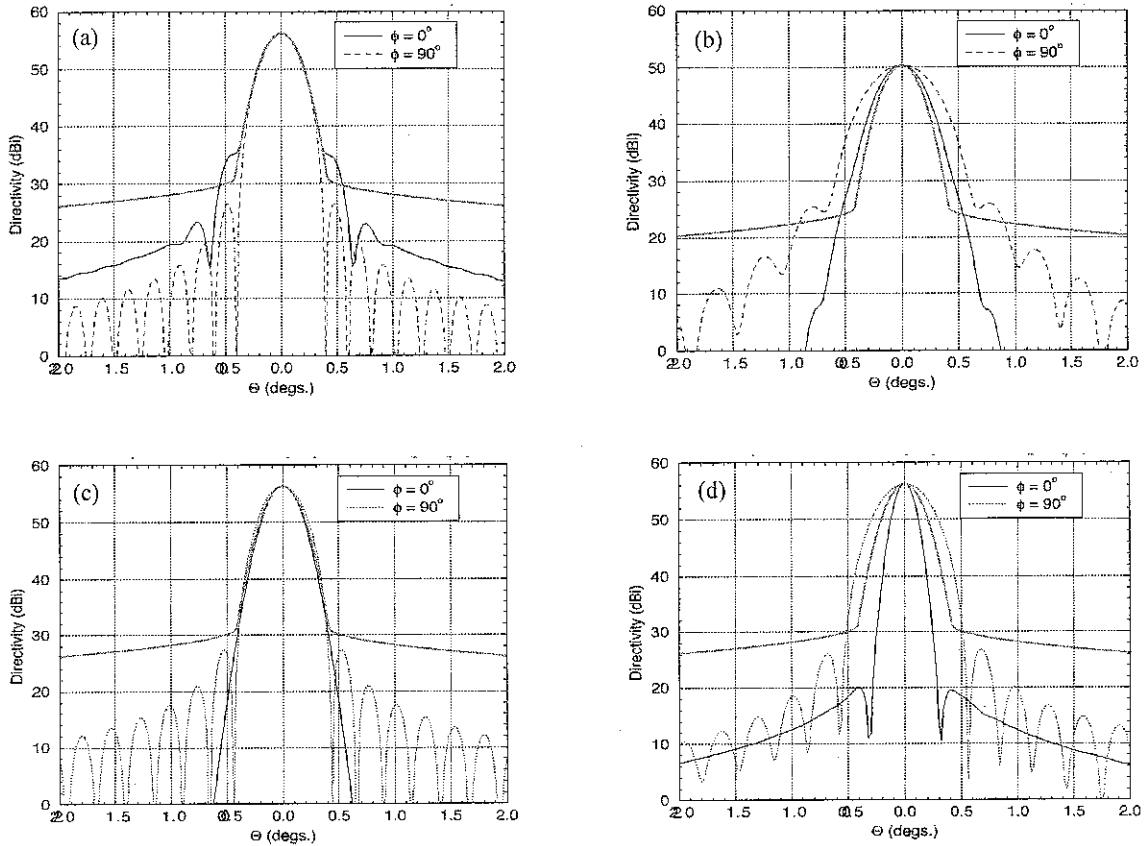


Fig. 7: Far-field directivity patterns in two principal planes. (a) 14 GHz, beam at boresight. (b) 14 GHz, beam tilt to 37°. (c) 35 GHz, beam at boresight. (d) 35 GHz, beam tilt to 37°. The desired sidelobe envelope template is also shown as green curves.

The mechanical design of the PR-2 antenna comprises a reflective membrane surface described as an offset parabolic cylinder of 5.3 m in length. The parabola has a linear (projected) span of 5.3 m originating at the apex, and a focal location at 1.89 m from the apex. A set of two precision chain links supported by inflatable and rigidizable tube booms will be used to deploy, pre-tension, and maintain the desired parabolic-cylindrical shape of the reflective membrane. The tube boom and chain link structure are cantilevered from the spacecraft interface and interconnected at their free ends by a rigid mandrel. This antenna mechanical configuration is shown in Figure 8. At launch, each chain link/boom is rolled up around a rigid mandrel, and the reflective membrane in turn, around the rigid cross-member; thus forming a cylindrical bundle with a launch volume no greater than a square cross section of 2 m x 2 m and 5.5 m in length. This antenna design is expected to have a mass density of less than 2.5 kg/m². In order to meet the low sidelobe requirement, the antenna's RMS surface accuracy should be better than 0.17 mm. To maintain such accuracy, the antenna must strive for a deployed fundamental frequency ≥ 0.5 Hz, the inflatable tube must be rigidized, and the reflective membrane must be dimensionally stable through the entire mission life in the expected space environments. Preliminary analyses and trade studies have been performed which indicate that these goals are achievable.

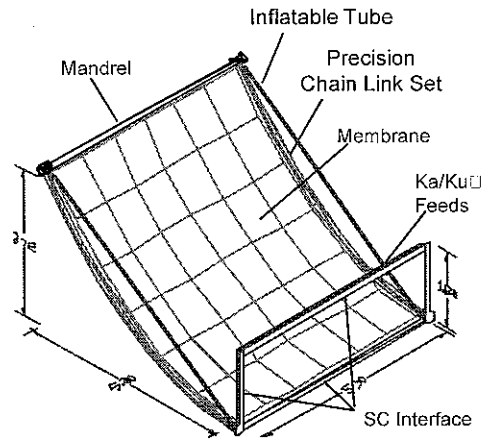


Fig. 8: PR-2 antenna's mechanical design concept.

3. GEO ATMOSPHERIC RADAR INSTRUMENT CONCEPT AND TECHNOLOGY

Concurrent to the LEO atmospheric radar study, the instrument concept and the associated technology roadmap for a notional GEO atmospheric radar are also being developed by NASA. The objective of the technology roadmap is to make use of the LEO PR-2 type technology to the extent possible, and at the same time identify the additional technology items that are unique and necessary for the eventual implementation of such a geostationary radar flight instrument.

The advantage of a space radar's ability to penetrate precipitating clouds relative to standard GOES cloud imagery is illustrated in Figure 9. This figure emphasizes how TRMM PR information can be used quantitatively to gauge the intensity of a hurricane, its vertical rain rate structure, and its water carrying capacity. It is also evident that the complete and frequent hurricane coverage by a geo-profiling radar will enable hurricane rain and cloud processes to be monitored over much of their life cycle, thus providing the temporal information needed for creating advanced flood and hazard warning systems, improving numerical model prediction of hurricane tracks and landfalls, and understanding more about the hurricane diurnal cycle. Furthermore, the cloud penetration ability of the radar will allow quantitative measurements of the vertical structures of both non-precipitating and precipitating clouds. This is of particular importance in addressing how cloud-radiation feedbacks and atmospheric hydrological cycle responds to external influences, such as deep ocean circulation induced warmings and coolings). The geostationary radar measurements, when used together with existing GOES measurements, can deduce vertical and horizontal cloud structure for the study and monitoring of solar and infrared radiative transfer in heterogeneous cloudy atmospheres, the essential ingredients for accurate diagnosis of the Earth's radiation budget and the atmosphere's radiative heating-cooling behavior. Since this radar approach is analogous to putting a NEXRAD system in orbit, it is being referred to as "NEXRAD in Space (NIS)".

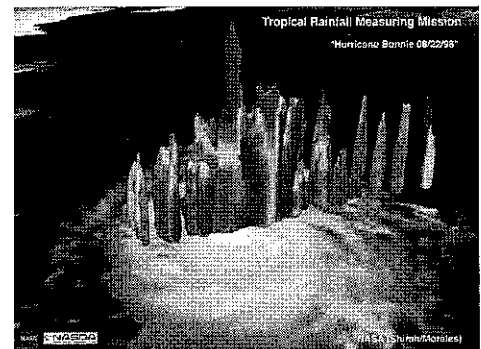


Fig. 9: TRMM PR acquired vertical rain profiles of Hurricane Bonnie overlaid on the corresponding GOES image.

3.1 NIS Observational Concept

NIS is designed to operate in the geostationary orbit at an altitude of 36,000 km. From the trade study between spatial resolution and rain penetration/profiling, we have selected 35 GHz as the radar frequency. A deployable, 30-m, spherical antenna reflector will be used together with two antenna feeds, one for signal transmission and the other for echo reception, to form the overall antenna subsystem. Both the reflector and the spacecraft will remain stationary as the antenna feeds perform spiral scans up to 4° from boresight to cover a 5300-km circular disk on the Earth surface. This coverage is equivalent to 48° ($\pm 24^\circ$) in both longitude and latitude. If necessary, small spacecraft maneuver can be used to extend the latitudinal coverage. This scan approach allows continuous and smooth transition between adjacent radar footprints. One complete disk scan will require 200 spirals. The NIS surface coverage is graphically illustrated in Figure 10, and the average time required for each spiral is given in Figure 11. The corresponding horizontal resolution ranges from 12 km at nadir to 14 km at 4° scan.

The dual-feed approach is used to compensate for the long range distance. The angular spacing between the transmit and receive feeds is designed to be 0.45° such that the rain echoes can be captured 0.25 seconds after pulse transmission. This approach also enables a two-fold increase in the number of radar echo samples obtained, which translates into a factor of 1.4 reduction in measurement noise. As the feeds scan through the spiral, the radar will continuously transmit radar pulses at a rate of 3.5 KHz. This selected rate will allow a vertical observation window of 25 km and will accommodate the range distance changes throughout the scans. The spiral scan rate as shown in Figure 11 is designed to obtain one full disk coverage within 60 minutes and to allow a constant dwell time on each radar resolution cell.

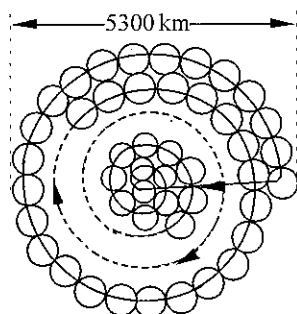


Fig. 10: Surface coverage by the spiral scan pattern.

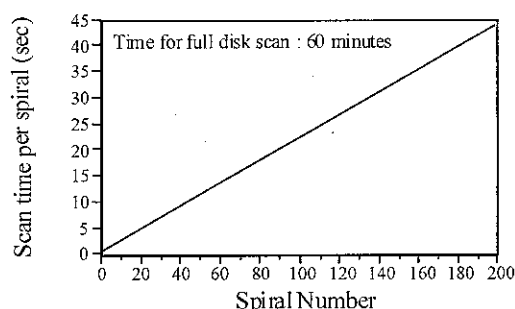


Fig. 11: Time per spiral (from inner-most to outer-most spiral).

3.2 NIS Instrument Parameters and Estimated Performance

The key NIS instrument and performance parameters are summarized in Table 2. Note that by an averaging of 120 pulses, the NIS detection sensitivity is improved to ~ 5 dBZ. The rain signal-to-noise ratios (SNRs) in Figure 12 show that NIS can indeed achieve significant rain penetration. For example, NIS can measure ~ 35 mm/hr rain down to 2.5 km from the cloud top. At higher rain rates, the attenuation become significant and NIS's penetration ability reduces.

Like all downward pointing precipitation radars, the NIS return signals from light rain can be contaminated by the simultaneous surface returns when the antenna is scanned away from nadir. However, since the rain rates associated with hurricanes and the 35-GHz rain attenuation are high, the surface clutter contamination is much less an issue than one might expect. To articulate this point, we computed the ratios of the rain signal to the combined noise and clutter (SNCR) at different rain rates. An example at 5 mm/hr rain over the ocean is shown in Figure 13. At or near nadir the SNCR is dominated by thermal noise. Between

Radar System Parameters			
Frequency	35 GHz	Bandwidth	0.58 MHz
Antenna diameter	33 m	Pulsewidth	100 μ sec
Ant. effective aperture	28 m	PRF	3.5 KHz
Ant. 3-dB beamwidth	0.019°	Power duty cycle	35%
Antenna gain	77.2 dBi	Transmit path loss	2 dB
Antenna sidelobe	-30 dB	Receive path loss	2 dB
Max. spiral scan angle	4°	Sys. Noise temp.	910 K
Time for a full scan	60 mins.	Dynamic range	70 dB
Peak power	100 W	Downlink data rate	155 Kbps
Performance Parameters			
Disk coverage diameter	5300 Km	Doppler precision	0.3 m/s
Vertical resolution	300 m	Pulse samples	120
Horiz. resolution (nadir)	12 Km	Min. Zeq (1 pulse)	15.4 dBZ
Horiz. resolution (4°)	14 Km	Min. Zeq (after ave)	5.0 dBZ

Table 2: NIS systems and performance parameters.

~5° and 15° incidence angles and at lower altitudes, the surface clutter becomes dominant. At larger incidence angles the clutter effect is reduced due to increased attenuation and weaker surface backscattering. The results thus show that at 5 mm/hr rain NIS can indeed penetrate down to lower than 2 km altitude at most incidence angles of interest. At larger rain rates the detectability is determined by attenuation and thermal noise, not clutter.

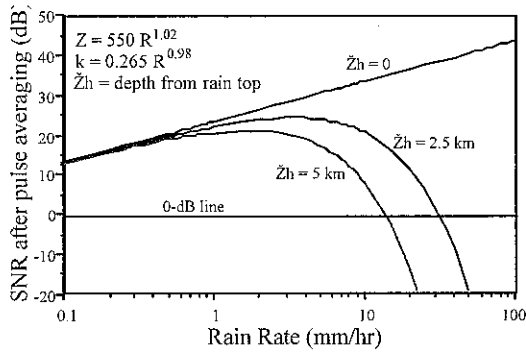


Fig. 12: SNRs for the NIS rain measurements.

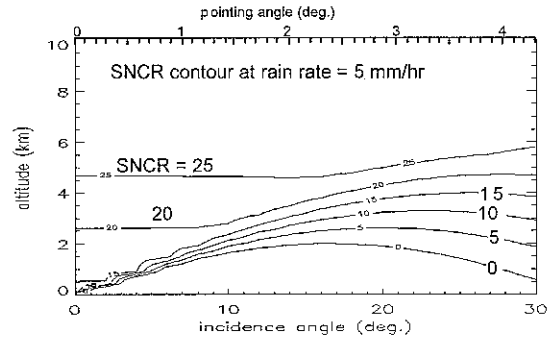


Fig. 13: SNCRs for the NIS at 5 mm/hr rain.

3.3 NIS Electronics

The NIS electronics design and functions are intended to mimic those of the PR-2 in order to leverage off the PR-2 electronics technology currently being developed. It consists of the RF electronics, digital electronics, and on-board processor. Since NIS requires only one transmitter and one receiver at 35 GHz, the functional requirements on the RF/digital electronics, as well as for the processor, will be significantly reduced. As such, the technology developed for the PR-2 electronics can be applied directly to NIS.

3.4 NIS Antenna Concept

NIS antenna requirements include an antenna gain of 77 dB, a beamwidth of 0.02°, a sidelobe level of lower than -30 dB, and a scan of up to 4° off its axis. This angular scan translates into a scan of ±200 beamwidths. The first potential antenna candidate is an electronically scanned array antenna. However, such a large array at 35 GHz would require over 6 million array elements. This is indeed a formidable and very expensive task. A second candidate is a parabolic reflector antenna. However, such antenna suffers from severe limitation at large beam scans. A focal plane array can potentially compensate for this performance degradation. Such implementation, however, necessitates the use of an active array with adaptively varying excitation coefficients for different look angles. Such an implementation could also be very expensive. The third candidate is a mechanically rotating antenna. For such a large antenna, the torque created by rotating the entire reflector will be very large. The fourth candidate is a spirally rotating spacecraft with a fixed-mounted antenna. This option can be very complicated and requires extensive interface between the radar and the spacecraft. For NIS, we focus on a novel spherical reflector antenna design⁵ which is capable of scanning its beams to any desired direction without compromise on the radiation performance. Any spherical aberration-induced degradation will be overcome by using a small planar array in the focal plane. Such a focal array can achieve any desired beam direction; more importantly, there is no need to reconfigure the array excitation coefficients for new beam direction.

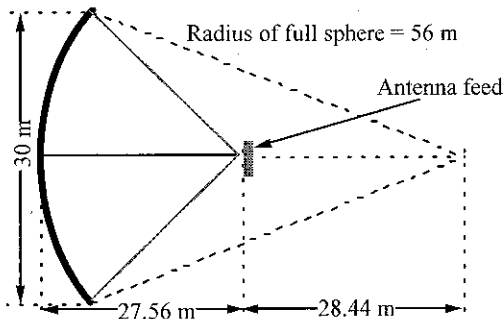


Fig. 14: Geometry of the NIS spherical reflector antenna.

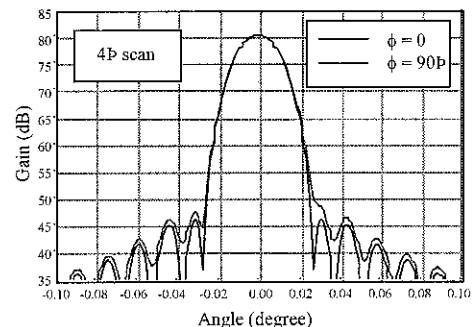


Fig. 15: NIS antenna patterns at 4° off-axis.

Spherical reflector antennas produce almost identical beams when their feeds are rotated with respect to the focal point. The major drawback is the excessive gain loss due to the presence of an extended focal region. Since the objective is to cover a $\pm 4^\circ$ angular range, we will use an oversized reflector antenna at 30m diameter to cover the desired angular range by utilizing sub-apertures for various beam look angles. This antenna configuration is graphical illustrated in Figure 14. Our initial parametric study showed that the utilization of a 271-element, rotating, fixed feed array with complex excitation coefficients would substantially improve the performance of the spherical reflector antenna. The size of the feed array is ~ 20 cm in diameter. The corresponding antenna radiation patterns at 4° scan are shown in Figure 15. Note that an antenna gain of ~ 80 dB with sidelobe levels below 30 dB are obtained.

The two feed arrays will be mechanically moved on a spiral track. One mechanism which achieves the desired motion is a rotating arm which carries a trolley containing the two feeds. The trolley travels along the axis of the arm on precision wheels preloaded against precision rails.

3.5 NIS Deployable Antenna Mechanical Design Concept

From mass and size considerations, three mechanical reflector concepts can potentially be adapted for the NIS antenna application. The first concept, shown in Figure 16(a), employs the emerging space inflatable technology. When deployed, the reflector assumes a lenticular shape formed by two spherical thin-film membrane halves. One of the membrane halves is coated and functions as the reflective surface. The other membrane half is a transparent canopy, with the sole function of holding the extremely low (about 10-4 psi) inflation pressure. A circular torus and three struts, all are made of membrane materials and are inflation deployable and space rigidizeable, provide structural support for the reflector. Ultra-flex solar arrays that have membrane substrates can be mounted on the surface of the torus. Development of flexible solar arrays with higher efficiency is currently being carried out mainly under the sponsorship of DoD. Based on ground measurements of a 14-m off-axis parabolic reflector developed for the Inflatable Antenna Experiment (IAE) launched with the shuttle mission in 1996, the best as-manufactured surface accuracy for an on-axis spherical inflatable reflector is expected to be in the range of 0.5 to 1 mm RMS. To further improve the surface accuracy, adaptive shape control can be used for on-orbit configuration adjustments.

The second design concept in Figure 16(b) uses the AstroMesh reflector approach. Structurally, this reflector consists of a cable-actuated synchronized parallelogram mechanism (that deploys the reflector) and a pair of ring-stiffened, tension-tied geodesic domes. The reflective mesh is stretched over the back of one of the domes. Based on the measured surface error of < 0.36 mm RMS on the Astro's 6-m flight model, and the consideration on several potential design improvements, including denser geodesic net structures, CTE tailoring, thinner webs, and refined materials conditioning, a 30-m AstroMesh reflector should meet the 0.75-mm RMS performance goal. Since sunrays can pass the mesh, traditional solid solar array panels attached to the spacecraft bus can be used for this option.

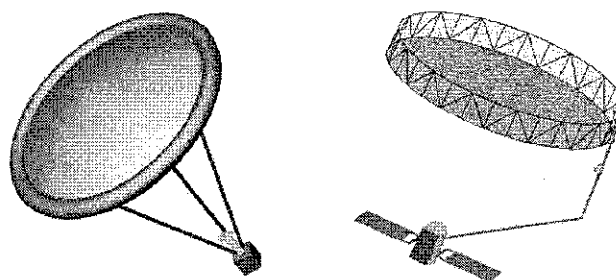


Fig. 16: (a) Inflatable reflector concept; (b) AstroMesh concept.

The third concept option is a hybrid of the first two concepts. It uses the mesh to deploy a reflective thin-film (less than 1 mil) antenna aperture for improved RF performance. In this case, the mesh can be made of thin lightweight wires and the grids of the mesh can be relatively coarse. With a slightly increased reflector diameter, an annular ring of ultra-flex membrane solar arrays can be incorporated around the antenna aperture to eliminate the need for traditional solid solar panels.

4. SUMMARY

This paper presents the conceptual designs and the technologies associated with the next-generation of atmospheric radars for remote sensing of precipitation from both the low-earth and geostationary orbits. In each case, several innovative design and technology features are being incorporated in order to enhance the rain measurement capability.

For the low earth orbiting PR-2 instrument, these innovative features include: 14/35-GHz dual-frequency operations, a large, shared-aperture, deployable, scanning antenna, dual-polarization, nadir Doppler measurements, pulse compression and real-time data processing, and instrument flexibility. It is anticipated that such instrument concept can provide significant data for advancing our understanding on rain processes, latent heating, climate variability, and atmospheric anomalies.

For the geostationary earth orbiting NIS instrument concept, the innovative features include a 35-GHz spirally scanning antenna feed set and a large, deployable spherical membrane antenna reflector. These combined features allowed the NIS instrument to acquire detailed information of the 3-dimensional structures of hurricanes, cyclones, and severe storms once every hour at 13-km horizontal resolution, 300-m vertical resolution, and 0.3-m/s precision in line-of-sight Doppler velocity.

ACKNOWLEDGMENTS

The research by the authors was performed by the Jet Propulsion Laboratory, California Institute of Technology, under contract with the National Aeronautics and Space Administration (NASA). The authors would like to acknowledge the supports provided by the Earth Science Instrument Incubator Program (IIP), the Tropical Rainfall Measuring Mission (TRMM) and the Global Precipitation Measurements (GPM) Mission of NASA.

REFERENCES

1. C. Kummerow, J. Simpson, O. Thiele, W. Barnes, A.T.C. Chang, E. Stocker, R. F. Adler, A. Hou, R. Kakar, E. Wentz, P. Ashcroft, T. Kouz, Y. Hong, K. Okamoto, T. Iguchi, H. Kuroiwa, E. Im, Z. Haddad, G. Huffman, B. Ferrier, W. S. Olson, E. Zipser, E. A. Smith, T. T. Wilheit, G. North, T. Krishnamurti, and K. Nakamura, "The status of the Tropical Rainfall Measuring Mission (TRMM) after 2 years in orbit," *J. Appl. Meteor.*, **39**, pp. 1965-1982, 2000.
2. T. Kozu, T. Kawanishi, H. Kuroiwa, M. Kojima, K. Oikawa, H. Kumagai, K. Okamoto, M. Okumura, H. Nakatsuka, and K. Nishikawa, "Development of precipitation radar onboard the Tropical Rainfall Measuring Mission (TRMM) satellite," *IEEE Trans. Geosci. Remote Sensing*, **GE-39**, pp. 102-43, 2001.
3. E.A. Smith, W.J. Adams, G.M. Flaming, S.P. Neek, and J.M. Shepherd, "The Global Precipitation Measurement (GPM) mission," *Mediterranean Storms 2001* (edited by R. Deidda, A. Mugnai, and F. Siccardi), 175-183, 2002.
4. S. L. Durden, E. Im, F.K. Li, W. Ricketts, A. Tanner, and W. Wilson, "ARMAR: An airborne rain mapping Radar," *J. Atmos. Oceanic Technol.*, **11**, pp. 727-737, 1994.
5. Y. Rahmat-Samii, "Improved reflector antenna performance using optimized feed arrays," *Proc. of 1989 URSI Intl. Sympos. on Electromagnetic Theory*, pp. 559-561, Stockholm, Sweden, August 14-17, 1989.